Journal of Machine Learning Research 0 (00) 0-00 Submitted 0/00; Published 00/00

Extrapolating expected accuracies for recognition tasks

Charles Zheng CHARLES.Y.ZHANG@GMAIL.COM
Department of Statistics
Stanford University
Palo Alto, CA

Rakesh Achanta
Department of Statistics
Stanford University
Palo Alto, CA

Yuval Benjamini YUVAL.BENJAMINI@MAIL.HUJI.AC.IL
Department of Statistics
The Hebrew University of Jerusalem,
Jerusalem, Israel

Editor: No One Yet

Abstract

The difficulty of multi-class classification generally increases with the number of classes. Using data from a subset of the classes, can we predict how well a classifier will scale with an increased number of classes? Under the assumption that the classes are sampled identically and independently from a population, and under the assumption that the classifier is based on independently learned scoring functions, we show that the expected accuracy when the classifier is trained on k classes is the $k-1$st moment of a certain distribution that can be estimated from data. We present an unbiased estimation method based on the theory, and demonstrate its application on a facial recognition example.

Keywords: Multiclass classification

1. Introduction

Many machine learning tasks are interested in recognizing or identifying an individual instance within a large set of possible candidates. These problems are usually modeled as multi-class classification problems, with a large and possibly complex label set. Leading examples include detecting the speaker from his voice patterns (Togneri and Pullella, 2011), identifying the author from her written text (Stamatatos et al., 2014), or labeling the object category from its image (Duygulu et al., 2002; Deng et al., 2010; Oquab et al., 2014). In all these examples, the algorithm observes an input x, and uses the classifier function h to guess the label y from a large label set $\mathcal{S}$.

There are multiple practical challenges in developing recognition systems for large label sets. Collecting high quality training data is perhaps the main obstacle, as the costs scale with the number of classes. It can be affordable to first collect data for a small set of classes, even if the long-term goal is to generalize to a larger set. Furthermore, classifier development can be accelerated by training first on fewer classes, as each training cycle may

require substantially less resources. Indeed, due to interest in how small-set performance generalizes to larger sets, such comparisons can found in the literature (Oquab et al., 2014; Griffin et al., 2007). A natural question is how does changing the size of the label set affect the classification accuracy?

Technically, we consider a pair of classification problems on finite label sets: a source task with label set $\mathcal{S}_{k_1}$ of size k_1, and a target task with a larger label set $\mathcal{S}_{k_2}$ of size $k_2 > k_1$. For each label set $\mathcal{S}_k$, one constructs the classification rule $h^{(k)} : \mathcal{X} \to \mathcal{S}_k$. Supposing that in each task, the test example (X^*, Y^*) has a joint distribution, define the generalization accuracy for label set $\mathcal{S}_k$ as

$$\mathrm{GA}_k = \Pr[h^{(k)}(X^*) = Y^*]. \tag{1}$$

The problem of *performance extrapolation* is the following: using data from only the source task $\mathcal{S}_{k_1}$, predict the accuracy for a target task with a larger unobserved label set $\mathcal{S}_{k_2}$.

A natural use case for performance extrapolation would be in the deployment of a facial recognition system. Suppose a system was developed in the lab on a database of k_1 individuals. Clients would like to deploy this system on a new larger set of k_2 individuals. Performance extrapolation could allow the lab to predict how well the algorithm will perform on the client's problem, accounting for the difference in label set size.

Extrapolation should be possible when the source and target classifications are two instances of a similar recognition problem. In many cases, the set of categories $\mathcal{S}$ is to some degree a random or arbitrary selection out of a larger, perhaps infinite, set of potential categories $\mathcal{Y}$. Yet any specific experiment uses a fixed finite set. For example, categories in the classical Caltech-256 image recognition dataset (Griffin et al., 2007) were assembled by aggregating keywords proposed by students and then collecting matching images from the web. The arbitrary nature of the label set is even more apparent in biometric applications (face recognition, authorship, fingerprint identification) where the labels correspond to human individuals (Togneri and Pullella, 2011; Stamatatos et al., 2014). In all these cases, the number of the labels used to define a concrete dataset is therefore an experimental choice rather than a property of the domain. Despite the arbitrary nature of these choices, such datasets are viewed as representing the larger problem of recognition within the given domain, in the sense that success on such a dataset should inform performance on similar problems.

In this paper, we assume that both $\mathcal{S}_{k_1}$ and $\mathcal{S}_{k_2}$ are independent identically distributed (i.i.d.) samples from a population (or distribution) of labels π, which is defined on the label space $\mathcal{Y}$. These assumptions help concretely analyze the generalization accuracy, although both are only approximate characterizations of the label selection process, which is often at least partially manual. Since we assume the label set is random, the generalization accuracy of a given classifier becomes a random variable. Performance extrapolation then becomes the problem of estimating the average generalization accuracy AGA_k of an i.i.d. label set $\mathcal{S}_k$ of size k. The condition of i.i.d. sampling of labels ensures that the separation of labels in a random set $\mathcal{S}_{k_2}$ can be inferred by looking at the empirical separation in $\mathcal{S}_{k_1}$, and therefore that some estimate of the average accuracy on $\mathcal{S}_{k_2}$ can be obtained. We also make the assumption that the classifiers train a separate model for each class. This convenient property allows us to characterize the accuracy of the classifier by selectively conditioning on one class at a time.

Our paper presents two main contributions related to extrapolation. First, we present a theoretical formula describing how average accuracy for smaller k is linked to average accuracy for label set of size $K > k$. We show that accuracy at any size depends on a *favorability* function D, which is determined by properties of the data distribution and the classifier. Second, we propose an estimation procedure that allows extrapolation of the observed average accuracy curve from k_1-class data to a larger number of classes, based on the theoretical formula. Under certain conditions, the estimation method has the property of being an unbiased estimator of the average accuracy.

The paper is organized as follows. In the rest of this section, we discuss related work. The framework of randomized classification is introduced in Section 2, and there we also introduce a toy example which is revisited throughout the paper. Section 3 develops our theory of extrapolation, and Section 3.3 we suggest an estimation method. In Section 5, we demonstrate our method on a facial recognition problem, making use of the OpenFace feature extraction network Amos et al. (2016). In Section 6 we discuss modeling choices and limitations of our theory, as well as potential extensions.

1.1 Related work

Linking performance between two different but related classification tasks can be considered an instance of transfer learning (Pan and Yang, 2010). Under Pan and Yang's terminology, our setup is an example of multi-task learning, because the source task has labeled data, which is used to predict performance on a target task that also has labeled data. Applied examples of transfer learning from one label set to another include Oquab et al. (2014), Donahue et al. (2014), Sharif Razavian et al. (2014). However, there is little theory for predicting the behavior of the learned classifier on a new label set. Instead, most research classification for large label sets deal with the computational challenges of jointly optimizing the many parameters required for these models for specific classification algorithms (Crammer and Singer, 2001; Lee et al., 2004; Weston et al., 1999). Gupta et al. (2014) presents a method for estimating the accuracy of a classifier which can be used to improve performance for general classifiers, but doesn't apply for different set sizes.

The theoretical framework we adopt is one where there exists a family of classification problems with increasing number of classes. This framework can be traced back to Shannon (1948), who considered the error rate of a random codebook, which is a special case of randomized classification. More recently, a number of authors have considered the problem of high-dimensional feature selection for multiclass classification with a large number of classes (Pan et al., 2016; Abramovich and Pensky, 2015; Davis et al., 2011). All of these works assume specific distributional models for classification compared to our more general setup. However, we do not deal with the problem of feature selection.

Perhaps the most similar method that deals with extrapolation of classification error to a larger number of classes can be found in Kay et al. (2008). They trained a classifier for identifying the observed stimulus from a functional MRI scan of brain activity, and were interested in its performance on larger stimuli sets. They proposed an extrapolation algorithm as a heuristic with little theoretical discussion. In Section 4 we interpret their method within the our theory, and discuss cases where it performs well compared to our algorithm.

2. Randomized classification

2.1 Setup

The randomized classification model we study has the following features. We assume that there exists an infinite, perhaps continuous, label space $\mathcal{Y}$ and a example space $\mathcal{X} \in \mathbb{R}^p$. We assume there exists a prior distribution π on the label space $\mathcal{Y}$. And for each label $y \in \mathcal{Y}$, there exists a distribution of examples F_y. In other words, for an example-label pair (X, Y), the conditional distribution of X given $Y = y$ is given by F_y.

A random classification task can be generated as follows. The label set $\mathcal{S} = \{Y^{(1)}, \ldots, Y^{(k)}\}$ is generated by drawing labels $Y^{(1)}, \ldots, Y^{(k)}$ i.i.d. from π. For each label, we sample a training set and a test set. The training set is obtained by sampling r_{train} observations $X^{(i)}_{j,train}$ i.i.d. from $F_{Y^{(i)}}$ for $j = 1, \ldots, r_{train}$ and $i = 1, \ldots, k$. The test set is likewise obtained by sampling r observations $X^{(i)}_j$ i.i.d. from $F_{Y^{(i)}}$ for $j = 1, \ldots, r$.

We assume that the classifier $h(x)$ works by assigning a score to each label $y^{(i)} \in \mathcal{S}$, then choosing the label with the highest score. That is, there exist real-valued *score functions* $m_{y^{(i)}}(x)$ for each label $y^{(i)} \in \mathcal{S}$. Since the classifier is allowed to depend on the training data, it is convenient to view it (and its associated score functions) as random. We write $H(x)$ when we wish to work with the classifier as a random function, and likewise $M_y(x)$ to denote the score functions when they are considered as random.

For a fixed instance of the classification task with labels $\mathcal{S} = \{y^{(i)}\}_{i=1}^k$ and associated score functions $\{m_{y^{(i)}}\}_{i=1}^k$, recall the definition of the k-class generalization error (1). Assuming that there are no ties, it can be written in terms of score functions as

$$\mathrm{GA}_k(h) = \frac{1}{k} \sum_{i=1}^{k} \Pr[m_{y^{(i)}}(X^{(i)}) = \max_j m_{y^{(j)}}(X^{(i)})],$$

where $X^{(i)} \sim F_{y^{(i)}}$ for $i = 1, \ldots, k$. However, when we consider the labels $\{Y^{(i)}\}_{i=1}^k$ and associated score functions to be random, the generalization accuracy also becomes a random variable.

Suppose we specify k but do not fix any of the random quantities in the classification task. Then the k-class *average generalization accuracy* of a classifier is the expected value of the generalization accuracy $\mathrm{GA}_k(H)$ resulting from a random set of k labels, $Y^{(1)}, \ldots, Y^{(k)} \overset{iid}{\sim} \pi$, and their associated score functions:

$$\begin{aligned} \mathrm{AGA}_k &= \frac{1}{k} \sum_{i=1}^{k} \Pr[M_{Y^{(i)}}(X^{(i)}) = \max_j M_{Y^{(j)}}(X^{(i)})] \\ &= \Pr[M_{Y^{(1)}}(X^{(1)}) = \max_j M_{Y^{(j)}}(X^{(1)})]. \end{aligned}$$

The last line follows from noting that all k summands in the previous line are identical. [The definition of average generalization accuracy is illustrated in Figure 1.]

2.1.1 Marginal classifier

In our analysis, we do not want the classifier to rely too strongly on complicated interactions between the labels in the set. We therefore propose the following property of marginal separability for classification models:

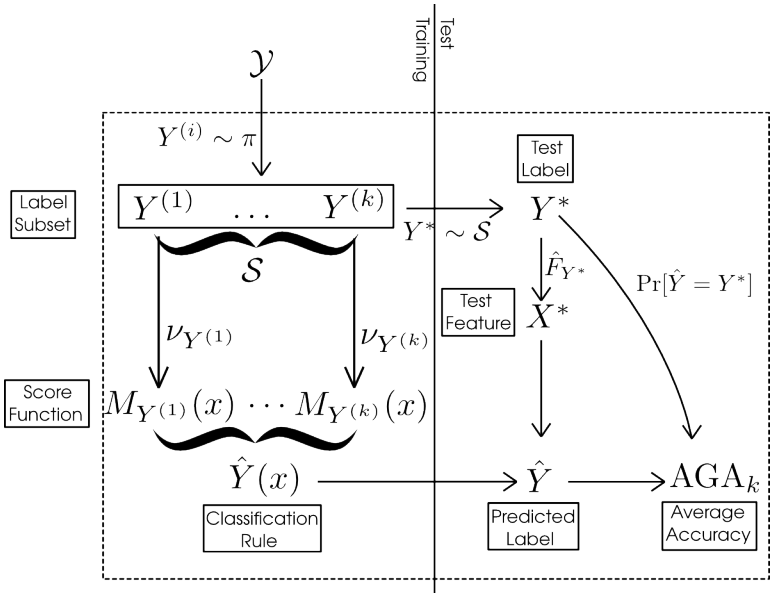

Figure 1: **Average generalization accuracy:** A diagram of the random quantities underlying the average generalization accuracy for k labels (AGA_k). At the training stage (left), a set of k labels $\mathcal{S}$ is sampled from the prior π, and score functions are trained from examples for these classes. At the test stage (right), one true class Y^* is sampled uniformly from $\mathcal{S}$, as well as a test example X^*. AGA_k measures the expected accuracy over these random variables.

Definition 1 *The classifier $H(x)$ is called a* marginal classifier *if the score function $M_{y^{(i)}}(x)$ only depends on the label $y^{(i)}$ and the class training set $X^{(i)}_{j,train}$.*

$$M_{y^{(i)}}(x) = g(x; y^{(i)}, X^{(i)}_{1,train}, ..., X^{(i)}_{r_{train},train})$$

This means that the score function for $y^{(i)}$ does not depend on other labels $y^{(j)}$ or their training samples. Therefore, each M_y can be considered to have been drawn from a distribution ν_y. Classes "compete" only through selecting the highest score, but not in constructing the score functions. The operation of a marginal classifier is illustrated in figure 2.

The *marginal* property allows us to prove strong results about the accuracy of the classifier under i.i.d. sampling assumptions.

Comments:

1. If H is a marginal classifier then $M_{Y^{(i)}}$ is independent of $Y^{(j)}$ and $M_{Y^{(j)}}$ for $i \neq j$.

2. Estimated Bayes classifiers are primary examples of marginal classifiers. Let $\hat{f}_y$ be a density estimate of the example distribution under label y obtained from the empirical distribution $\hat{F}_y$. Then, we can use the estimated density to produce the score functions:

$$m^{EB}_y(x) = \log(\hat{f}_y(x)).$$

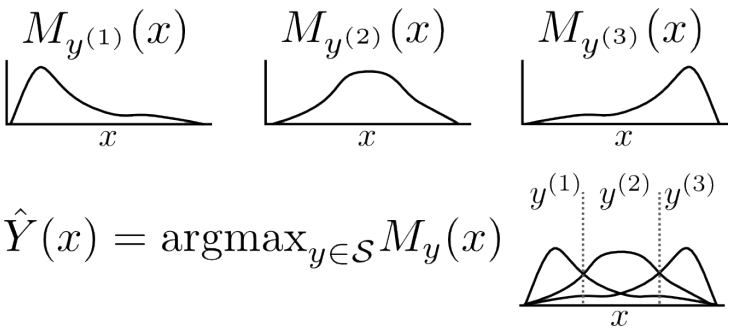

Figure 2: **Classification rule:** Top: Score functions for three classes for a one-dimensional example space. Bottom: The classification rule chooses between $y^{(1)}, y^{(2)}$ or $y^{(3)}$ by choosing the maximal score function.

The resulting empirical approximation for the Bayes classifier would be

$$h^{EB}(x) = \text{argmax}_{y \in \mathcal{S}}(m_y^{EB}(x)).$$

3. Both the Quadratic Discriminant Analysis and the naive Bayes classifiers can be seen as specific instances of an estimated Bayes classifier [1]. For QDA, the score function is given by

$$m_y^{QDA}(x) = -(x - \mu(\hat{F}_y))^T \Sigma(\hat{F}_y)^{-1}(x - \mu(\hat{F}_y)) - \log\det(\Sigma(\hat{F}_y)),$$

where $\mu(F) = \int y dF(y)$ and $\Sigma(F) = \int (y - \mu(F))(y - \mu(F))^T dF(y)$. In Naive Bayes, the score function is

$$m_y^{NB}(x) = \sum_{j=1}^{p} \log \hat{f}_{y,j}(x),$$

where $\hat{f}_{y,j}$ is a density estimate for the j-th component of $\hat{F}_y$.

4. For some classifiers, M_y is a deterministic function of y (and therefore ν_y is degenerate). A prime example is when exists fixed or pre-trained embeddings $g, \tilde{g}$ that map labels y and examples x into R^p. Then

$$M_y^{embed} = -\|g(y) - \tilde{g}(x)\|_2. \tag{2}$$

This describes, for example, a 1-nearest neighbor classifier.

5. There are many classifiers which do not satisfy the marginal property, such as multinomial logistic regression, multilayer neural networks, decision trees, and k-nearest neighbors.

1. QDA is the special case of the estimated Bayes classifier when $\hat{f}_y$ is obtained as the multivariate Gaussian density with mean and covariance parameters estimated from the data. Naive Bayes is the estimated Bayes classifier when $\hat{f}_y$ is obtained as the product of estimated componentwise marginal distributions of $p(x_i|y)$

Notational remark. Henceforth, we shall relax the assumption that the classifier $H(x)$ is based on a training set. Instead, we assume that there exist score functions $\{M_{Y^{(i)}}\}_{i=1}^{k}$ associated with the random label set $\{Y^{(i)}\}_{i=1}^{k}$, and that the score functions $M_{Y^{(i)}}$ are independent of the test set. The classifier $H(x)$ is marginal if and only if $M_{Y^{(i)}}$ are independent of both $Y^{(j)}$ and $M_{Y^{(j)}}$ for $j \neq i$.

2.2 Estimation of average accuracy

Before tackling extrapolation, it is useful to discuss a simpler task of generalizing accuracy results when the target set is *not* larger than the source set. Suppose we have test data for a classification task with k_1 classes. That is, we have a label set $\mathcal{S}_{k_1} = \{y^{(i)}\}_{i=1}^{k_1}$ and its associated set of score functions $M_{y^{(i)}}$, as well as test observations $(x_1^{(i)}, \ldots, x_r^{(i)})$ for $i = 1, \ldots, k_1$. What would be the predicted accuracy for a new randomly sampled set of $k_2 \leq k_1$ labels?

Note that AGA_{k_2} is the expected value of the accuracy on the new set of k_2 labels. Therefore, any unbiased estimator of AGA_{k_2} will be an unbiased predictor for the accuracy on the new set.

Let us start with the case $k_2 = k_1 = k$. For each test observation $x_j^{(i)}$, define the ranks of the candidate classes $\ell = 1, \ldots, k$ by

$$R_j^{i,\ell} = \sum_{s=1}^{k} I\{m_{y^{(\ell)}}(x_j^{(i)}) \geq m_{y^{(s)}}(x_j^{(i)})\}.$$

The test accuracy is the fraction of observations for which the correct class also has the highest rank

$$\mathrm{TA}_k = \frac{1}{rk} \sum_{i=1}^{k} \sum_{j=1}^{r} I\{R_j^{i,i} = k\}. \tag{3}$$

Taking expectations over both the test set and the random labels, the expected value of the test accuracy is AGA_k; hence, TA_k provides the desired estimator.

Next, let us consider the case where $k_2 < k_1$. Consider label set $\mathcal{S}_{k_2}$ obtained by sampling k_2 labels uniformly without replacement from $\mathcal{S}_{k_1}$. Since $\mathcal{S}_{k_2}$ is unconditionally an i.i.d. sample from the population of labels π, the test accuracy of $\mathcal{S}_{k_2}$ is an unbiased estimator of AGA_{k_2}. However, we can get a better unbiased estimate of AGA_{k_2} by averaging over all the possible subsamples $\mathcal{S}_{k_2} \subset \mathcal{S}_{k_1}$. This defines the average test accuracy over subsampled tasks, ATA_{k_2}.

Remark. Naïvely, computing ATA_{k_2} requires us to train and evaluate $\binom{k_1}{k_2}$ classification rules. However, for marginal classifiers, retraining the classifier is not necessary. Looking at the rank $R_j^{i,i}$ of the correct label i for $x_j^{(i)}$, allows us to determine how many subsets $\mathcal{S}_2$ will result in a correct classification. Specifically, there are $R_j^{i,i} - 1$ labels with a lower score than the correct label i. Therefore, as long as one of the classes in $\mathcal{S}_2$ is i, and the other $k_2 - 1$ labels are from the set of $R_j^{i,i} - 1$ labels with lower score than i, the classification of $x_j^{(i)}$ will be correct. This implies that there are $\binom{R_j^{i,i}-1}{k_2-1}$ such subsets $\mathcal{S}_2$ where $x_j^{(i)}$ is

classified correctly, and therefore the average test risk for all $\binom{k_1}{k_2}$ subsets $\mathcal{S}_2$ is

$$\mathrm{ATA}_{k_2} = \frac{1}{\binom{k_1}{k_2}} \frac{1}{rk_2} \sum_{i=1}^{k_1} \sum_{j=1}^{r} \binom{R_j^{i,i} - 1}{k_2 - 1}. \tag{4}$$

2.3 Toy Example: Bivariate normals

Let us illustrate these ideas using a toy example. Let (Y, X) have a bivariate normal joint distribution,

$$(Y, X) \sim N\left(\begin{pmatrix}0\\0\end{pmatrix}, \begin{pmatrix}1 & \rho\\ \rho & 1\end{pmatrix}\right),$$

as illustrated in figure 3(a). Therefore, for a given randomly drawn label Y, the conditional distribution of X for that label is univariate normal with mean ρY and variance $1 - \rho^2$:

$$X|Y = y \sim N(\rho Y, 1 - \rho^2).$$

Supposing we draw $k = 3$ labels y_1, y_2, y_3, the classification problem will be to assign a test instance X^* to the correct label. The test instance X^* would be drawn with equal probability from one of three conditional distributions $X|Y = y^{(i)}$, as illustrated in figure 3(b, top). The Bayes rule assigns X^* to the class with the highest density $p(x|y_i)$, as illustrated by figure 3(b, bottom): it is therefore a marginal classifier, with score function

$$M_{y^{(i)}}(x) = \log(p(x|y^{(i)})) = -\frac{(x - \rho y)^2}{2(1 - \rho^2)} + \text{const.}$$

For this model, the generalization accuracy of the Bayes rule for any label set $\{y^{(1)}, \ldots, y^{(k)}\}$ is given by

$$\begin{aligned}\mathrm{GA}_k(y_1, \ldots, y_k) &= \frac{1}{k} \sum_{i=1}^{k} \Pr_{X \sim p(x|y_i)}[p(X|y_i) = \max_{j=1}^{k} p(X|y_j)] \\ &= \frac{1}{k} \sum_{i=1}^{k} \Phi\left(\frac{y^{[i+1]} - y^{[i]}}{2\sqrt{1 - \rho^2}}\right) - \Phi\left(\frac{y^{[i-1]} - y^{[i]}}{2\sqrt{1 - \rho^2}}\right)\end{aligned}$$

where Φ is the standard normal cdf, $y^{[1]} < \cdots < y^{[k]}$ are the sorted labels, and $y^{[0]} = -\infty$ and $y^{[k+1]} = \infty$. We numerically computed $\mathrm{GA}_k(y_1, \ldots, y_k)$ for randomly drawn labels $Y_1, \ldots, Y_k \overset{iid}{\sim} N(0, 1)$; the distributions of GA_k for $k = 2, \ldots, 10$ are illustrated in figure 4. The mean of the distribution of GA_k is the k-class average risk, AGA_k. The theory presented in the next section deals with how to analyze the average risk AGA_k as a function of k.

3. Extrapolation

The section is organized as follows. We begin by introducing an explicit formula for the average accuracy AGA_k. The formula reveals that AGA_k is determined by moments of a one-dimensional function $D(u)$. Through this formula, therefore, we can infer through

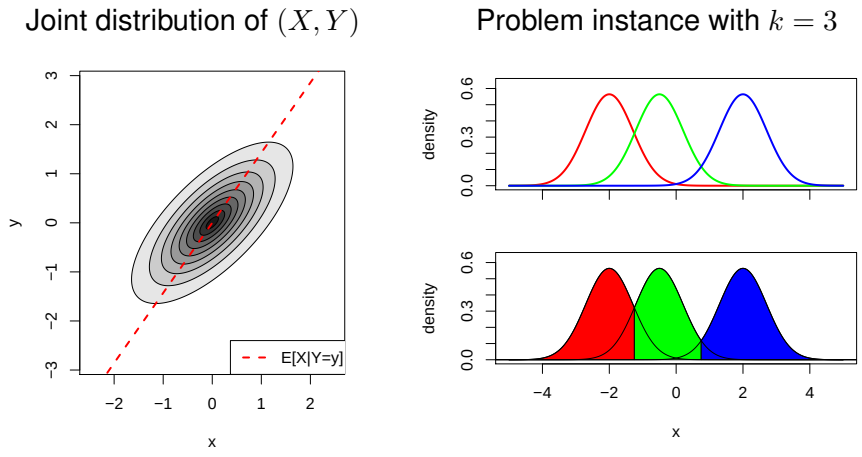

(a) (b)

Figure 3: **Toy example:** *Left:* The joint distribution of (X, Y) is bivariate normal with correlation $\rho = 0.7$. *Right:* A typical classification problem instance from the bivariate normal model with $k = 3$ classes. *(Top):* the conditional density of X given label Y, for $Y = \{y^{(1)}, y^{(2)}, y^{(3)}\}$. *(Bottom):* the Bayes classification regions for the three classes.

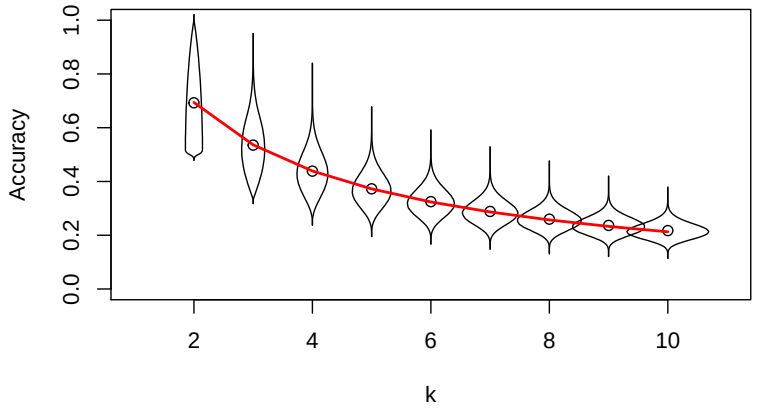

Figure 4: **Generalization accuracy for toy example:** The distribution of the generalization accuracy for $k = 2, 3, \ldots, 10$ for the bivariate normal model with $\rho = 0.7$. Circles indicate the average generalization accuracy AGA_k; the red curve is the theoretically computed average accuracy.

subsample accuracies estimates of $D(u)$. These estimates allow us to extrapolate the average generalization accuracy to an arbitrary number of labels.

The result of our analysis is to expose the average accuracy AGA_k as the weighted average of a function $D(u)$, where $D(u)$ is independent of k, and where k only changes the weighting. The result is stated as follows.

Theorem 2 *Suppose π, $\{F_y\}_{y\in\mathcal{Y}}$ and score functions M_y satisfy the tie-breaking condition. Then, there exists a cumulative distribution function $D(u)$ defined on the interval $[0,1]$ such that*

$$AGA_k = 1 - (k-1)\int D(u)u^{k-2}du. \tag{5}$$

The tie-breaking allows us to neglect specifying the case when margins are tied.

Definition 3 Tie-breaking condition*: for all $x \in \mathcal{X}$, $M_Y(x) \neq M_{Y'}(x)$ with probability one for Y, Y' independently drawn from π.*

In practice, one can simply break ties randomly, which is mathematically equivalent to adding a small amount of random noise ϵ to the function $\mathcal{M}$.

3.1 Analysis of average accuracy

For the following discussion, we often consider a random label with its associated score function and example vector. Explicitly, this sampling can be written:

$$Y \sim \pi,\ M_Y|Y \sim \nu_Y,\ X|Y \sim F_Y.$$

Similarly we use $(Y', M_{Y'}, X')$ and (Y^*, M_{Y^*}, X^*) for two more triplets with independent and identical distributions. Specifically, X^* will typically note the test example, and therefore Y^* the true label and M_{Y^*} its score function.

The function D is related to a favorability function. Favorability measures the probability that the score for the example x^* is going to be maximized by the score function m_y, compared to a random competitor $M_{Y'}$. Formally, we write:

$$U_{x^*}(m_y) = \Pr[m_y(x^*) > M_{Y'}(x^*)]. \tag{6}$$

Note that for fixed example x^*, favorability is monotonically increasing in $m_y(x^*)$. If $m_y(x^*) > m_{y^\dagger}(x^*)$, then $U_{x^*}(y) > U_{x^*}(y^\dagger)$, because the event $\{m_y(x^*) > M_{Y'}(x^*)\}$ contains the event $\{m_{y^\dagger}(x^*) > M_{Y'}(x^*)\}$.

Therefore, given labels $y^{(1)}, \ldots, y^{(k)}$ and test instance x^*, we can think of the classifier as choosing the label with the greatest favorability:

$$\hat{y} = \mathrm{argmax}_{y^{(i)}\in\mathcal{S}} m_{y^{(i)}}(x^*) = \mathrm{argmax}_{y^{(i)}\in\mathcal{S}} U_{x^*}(m_{y^{(i)}}).$$

Furthermore, via a conditioning argument, we see that this is still the case even when the test instance and labels are random:

$$\hat{Y} = \mathrm{argmax}_{Y^{(i)}\in\mathcal{S}} M_{Y^{(i)}}(X^*) = \mathrm{argmax}_{Y^{(i)}\in\mathcal{S}} U_{X^*}(M_{Y^{(i)}}).$$

The favorability takes values between 0 and 1, and when any of its arguments are random, it becomes a random variable with a distribution supported on $[0,1]$. In particular, we consider the following two random variables:

a. the *incorrect-label* favorability $U_{x^*}(M_Y)$ between a given fixed test instance x^*, and the score function of a random incorrect label M_Y, and

b. the *correct-label* favorability $U_{X^*}(M_{Y^*})$ between a random test instance X^*, and the score function of the correct label, M_{Y^*}.

3.1.1 Incorrect-label favorability

The incorrect-label favorability can be written explicitly as

$$U_{x^*}(M_Y) = \Pr[M_Y(x^*) > M_{Y'}(x^*)|M_Y]. \tag{7}$$

Note that M_Y and $M_{Y'}$ are identically distributed, and are both are unrelated to x^* that is fixed. This leads to the following result:

Lemma 4 *Under the tie-breaking condition, the incorrect-label favorability $U_{x^*}(M_Y)$ is uniformly distributed for any $x^* \in \mathcal{X}$, and*

$$\Pr[U_{x^*}(M_Y) \leq u] = u. \tag{8}$$

Proof is in the appendix.

3.1.2 Correct-label favorability

The correct-label favorability is

$$U^* = U_{X^*}(M_{Y^*}) = \Pr[M_{Y^*}(X^*) > M'_{Y'}(X^*)|Y^*, M_{Y^*}, X^*]. \tag{9}$$

The distribution of U^* will depend on π, F_y and ν_y, and generally cannot be written in a closed form. However, this distribution is central to our analysis–indeed, we will see that the function D appearing in theorem 2 is defined as the cumulative distribution function of U^*.

The special case of $k = 2$ shows the relation between the distribution of U^* and the average generalization accuracy, AGA_2. In the two-class case, the average generalization accuracy is the probability that a random correct label score function gives a larger value than a random distractor:

$$\mathrm{AGA}_2 = \Pr[M_{Y^*}(X^*) > M_{Y'}(X^*)].$$

where Y^* is the correct label, and Y' is a random incorrect label. If we condition on $Y^* = y^*$, $M_{Y^*} = m_{y^*}$ and $X^* = x^*$, we get

$$\mathrm{AGA}_2 = \mathbf{E}[\Pr[M_{Y^*}(X^*) > M_{Y'}(X^*)|Y^*, M_{Y^*}, X^*]].$$

Here, the conditional probability inside the expectation is the correct-label favorability. Therefore,

$$\mathrm{AGA}_2 = \mathbf{E}[U^*] = \int D(u)du,$$

where $D(u)$ is the cumulative distribution function of U^*, $D(u) = \Pr[U^* \leq u]$. Theorem 2 extends this to general k; we now give the proof.

Proof of Theorem 2.

Without loss of generality, suppose that the true label is Y^* and the incorrect labels are $Y^{(1)}, \ldots, Y^{(k-1)}$. We have

$$\text{AGA}_k = \Pr[M_{Y^*}(X^*) > \max_{i=1}^{k-1} M_{Y^{(i)}}(X^*)] = \Pr[U^* > \max_{i=1}^{k-1} U_{X^*}(M_{Y^{(i)}})]$$

recalling that $U^* = U_{X^*}(M_{Y^*})$. Now, if we condition on $X^* = x^*$, $Y^* = y^*$ and $M_{Y^*} = m_{y^*}$, then the random variable U^* becomes fixed, with value

$$u^* = U_{x^*}(m_{y^*}).$$

Therefore,

$$\begin{aligned}\text{AGA}_k &= \mathbf{E}[\Pr[U^* > \max_{i=1}^{k-1} U_{X^*}(M_{Y^{(i)}})|X^* = x^*, Y^* = y^*, M_{Y^*} = y^*]] \\ &= \mathbf{E}[\Pr[U^* > \max_{i=1}^{k-1} U_{X^*}(M_{Y^{(i)}})|X^* = x^*, U^* = u^*]]\end{aligned}$$

Now define $U_{max,k-1} = \max_{i=1}^{k-1} U_{X^*}(M_{Y^{(i)}})$. Since by Lemma 4, $U_{X^*}(M_{Y^{(i)}})$ are i.i.d. uniform conditional on $X^* = x^*$, we know that

$$U_{max,k-1}|X^* = x^* \sim \text{Beta}(k-1, 1). \tag{10}$$

Furthermore, $U_{max,k-1}$ is independent of U^* conditional on X^*. Therefore, the conditional probability can be computed as

$$\Pr[U^* > U_{max,k-1}|X^* = x^*, U^* = u^*] = \int_{u^*}^1 (k-1)u^{k-2}du.$$

Consequently,

$$\begin{aligned}\text{AGA}_k &= \mathbf{E}[\Pr[U^* > \max_{i=1}^{k-1} U_{x^*}(M_{Y^{(i)}})|X^* = x^*, U^* = u^*]] \\ &= \mathbf{E}[\int_0^{U^*} (k-1)u^{k-2}du|U^* = u^*] \\ &= \mathbf{E}[\int_0^1 I\{u \le U^*\}(k-1)u^{k-2}du] \\ &= (k-1)\int_0^1 \Pr[U^* \ge u]u^{k-2}du.\end{aligned}$$

Or equivalently,

$$\text{AGA}_k = 1 - (k-1)\int D(u)u^{k-2}du.$$

where $D(u)$ denotes the cumulative distribution function of U^* on $[0, 1]$:

$$D(u) = \Pr[U_{X^*}(M_{Y^*}) \le u]. \tag{11}$$

□.

Theorem 2 expresses the average accuracy as a weighted integral of the function $D(u)$. Having this theoretical result allows us to understand how the expected k-class risk scales with k in problems where all the relevant densities are known. However, applying this result in practice to estimate AGA_k requires some means of estimating the unknown function D– which we discuss in the section ?.

3.2 Favorability and average accuracy for the toy example

Recall that for the toy example from Section 2.3, the score function M_y was a non-random function of y that measures the distance between x and ρy

$$M_y(x^*) = \log(p(x^*|y)) = -\frac{(x^* - \rho y)^2}{2(1-\rho^2)}$$

For this model, the favorability function $U_{x^*}(m_y)$ compares the distance between x^* and ρy to the distance between x^* and $\rho Y'$ for a randomly chosen distractor $Y' \sim N(0,1)$:

$$\begin{aligned} U_{x^*}(m_y) &= \Pr[|\rho y - x^*| > |\rho Y' - x^*|] \\ &= \Phi\left(\frac{x^* + |\rho y - x^*|}{\rho}\right) - \Phi\left(\frac{x^* - |\rho y - x^*|}{\rho}\right), \end{aligned}$$

where Φ is the standard normal cumulative distribution function. Figure 5(a) illustrates the level sets of the function $U_{x^*}(m_y)$. The highest values of $U_{x^*}(m_y)$ are near the line $x^* = \rho y$ corresponding the to conditional mean of $X|Y$: as one moves farther from the line, $U_{x^*}(m_y)$ decays. Note however that large values of x^* and y (with the same sign) result in larger values of $U_{x^*}(m_y)$ since it becomes unlikely for $Y' \sim N(0,1)$ to exceed $Y = y$.

Using the formula above, we can calculate the correct-label favorability $U^* = U_{X^*}(M_{Y^*})$ and its cumulative distribution function $D(u)$. The function D is illustrated in figure 5(b) for the current example with $\rho = 0.7$. The red curve in figure 4 was computed using the formula

$$\text{AGA}_k = 1 - (k-1)\int D(u)u^{k-2}du.$$

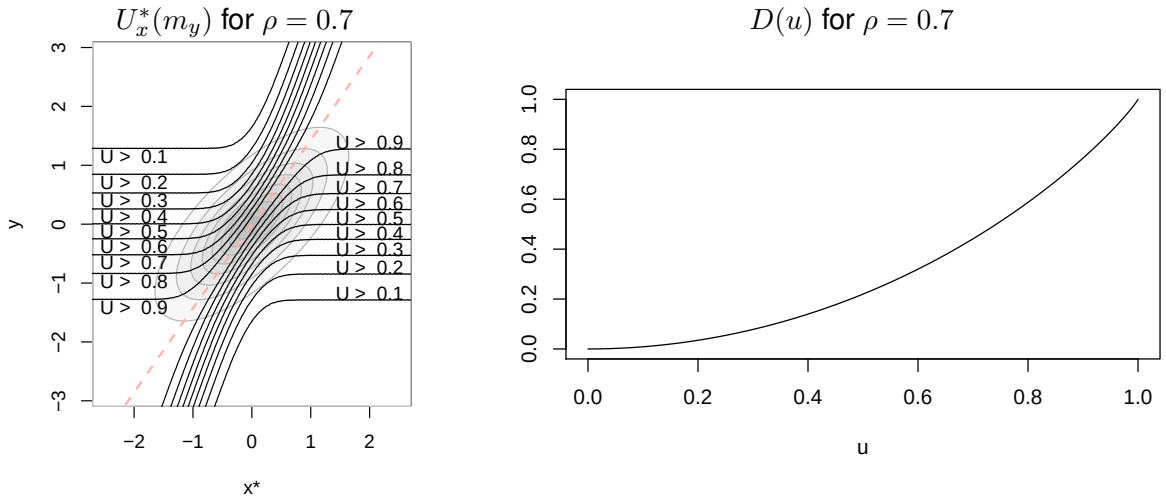

Figure 5: **Favorability for toy example:** *Left:* The level curves of the function $U_{x^*}(m_y)$ in the bivariate normal model with $\rho = 0.7$. *Right:* The function $D(u)$ gives the cumulative distribution function of the random variable $U_{X^*}(M_Y)$.

It is illuminating to consider how the average accuracy curves and the $D(u)$ functions vary as we change the parameter ρ. Higher correlations ρ lead to higher accuracy, as seen in figure 6(a), where the accuracy curves are shifted upward as ρ increases from 0.3 to 0.9. The favorability $U_{x^*}(m_y)$ tends to be higher on average as well, which leads to lower values of the cumulative distribution function–as we see in figure 6(b), where the function $D(u)$ becomes smaller as ρ increases.

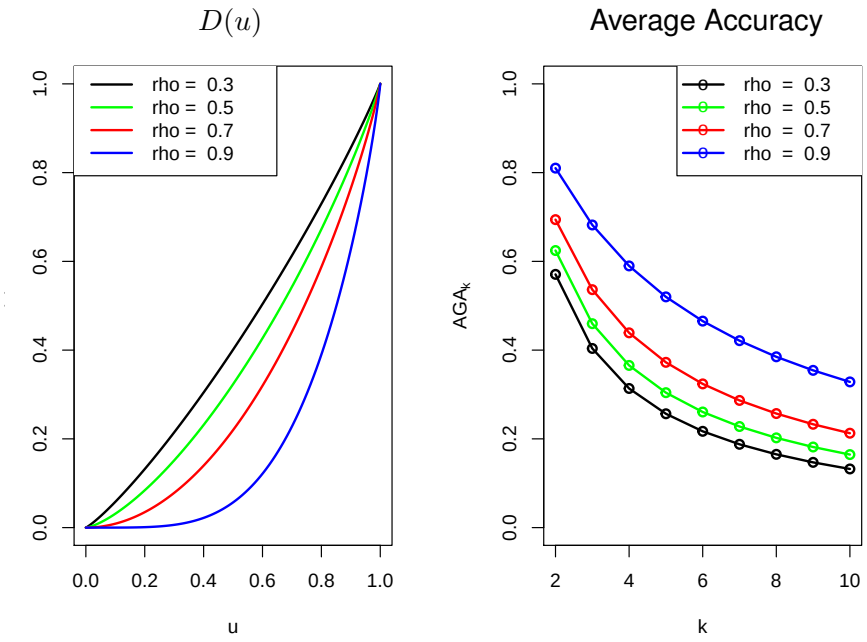

Figure 6: **Average accuracy with different ρ's:** *Left:* The average accuracy AGA_k. *Right:* $D(u)$ function for the bivariate normal model with $\rho \in \{0.3, 0.5, 0.7, 0.9\}$.

3.3 Estimation

Next, we discuss how to use data from smaller classification tasks to extrapolate average accuracy. Assume that we have data from a k_1-class random classification task, and would like to estimate the average accuracy AGA_{k_2} for $k_2 > k_1$ classes. Our estimation method will use the k-class average test accuracies, $\text{ATA}_2, ..., \text{ATA}_{k_1}$ (see Eq 4), for its inputs.

The key to understanding the behavior of the average accuracy AGA_k is the function D. We adopt a linear model

$$D(u) = \sum_{\ell=1}^{m} \beta_\ell h_\ell(u), \tag{12}$$

where $h_\ell(u)$ are known basis functions, and β_ℓ are the linear coefficients to be estimated. Since our proposed method is based on the linearity assumption (12), we call it the *regression method* for extrapolation.

Conveniently, the AGA_k can also be expressed in terms of the β_ℓ coefficients. If we plug in the assumed linear model (12) into the identity (5), then we get

$$1 - \mathrm{AGA}_k = (k-1) \int D(u) u^{k-2} du \tag{13}$$

$$= (k-1) \int_0^1 \sum_{\ell=1}^{m} \beta_\ell h_\ell(u) u^{k-2} du \tag{14}$$

$$= \sum_{\ell=1}^{m} \beta_\ell H_{\ell,k} \tag{15}$$

where

$$H_{\ell,k} = (k-1) \int_0^1 h_\ell(u) u^{k-2} du. \tag{16}$$

The constants $H_{\ell,k}$ are moments of the basis function h_ℓ: hence we call this method the *moment method.* Note that $H_{\ell,k}$ can be precomputed numerically for any $k \geq 2$.

Now, since the test accuracies ATA_k are unbiased estimates of AGA_k, this implies that the regression estimate

$$\hat{\beta} = \mathrm{argmin}_\beta \sum_{k=2}^{k_1} \left((1 - \mathrm{ATA}_k) - \sum_{\ell=1}^{m} \beta_\ell H_{\ell,k} \right)^2$$

is unbiased for β. The estimate of AGA_{k_2} is similarly obtained from (15), via

$$\widehat{\mathrm{AGA}_{k_2}} = 1 - \sum_{\ell=1}^{m} \hat{\beta}_\ell H_{\ell,k_2}. \tag{17}$$

3.4 Model selection

Accurate extrapolation using the regression method depends on a good fit between the linear model (12) and the true discriminability function $D(u)$. However, since the function $D(u)$ depends on the unknown joint distribution of the data, it makes sense to let the data help us choose a good basis $\{h_u\}$ from a set of candidate bases.

Extending the analogy between the regression method for prediction extrapolation and the well-studied problem of using regression to predict out-of-sample, we consider using *cross-validation* for model selection (Hastie et al., 2009). However, it is necessary to adjust the cross-validation procedure because of two particular differences betweem the usual prediction problem and the problem of prediction extrapolation: (i) while cross-validation is motivated for a setup with i.i.d. training and test data, in prediction extrapolation the the training data (the average test accuracies) are in fact highly corrrelated, and (ii) in prediction extrapolation, we know that the prediction is to be made in a particular direction (extrapolating to large k). Therefore, we use deterministic splits to minimize the dependence between the folds, splitting the training data into two halves: the first half consisting of $\{\mathrm{ATA}_2, \ldots, \mathrm{ATA}_{\lfloor k_1/2 \rfloor}\}$ and the second half consisting of $\{\mathrm{ATA}_{\lfloor k_1/2 \rfloor + 1}, \ldots, \mathrm{ATA}_{k_1}\}$. Furthermore, since we are only interested in how well the models *extrapolate* from small numbers of classes to a larger number of classes, and not in any other direction of prediction, we train

on the first half of the data and only predict on the held-out point ATA_{k_1} in the second half of the data[2] to evaluate cross-validation accuracy. Then, using ATA_{k_1} as the ground truth, we choose the basis that yields the closest prediction for $\hat{\mathrm{AGA}}_{k_1}$ in terms of absolute difference.

4. Simulation study

We ran simulations to check how the proposed extrapolation method performs in different settings. The results are displayed in Figure 7. We varied the number of classes k_1 in the source dataset, the difficulty of classification, and the basis functions. We generated data according to a mixture of isotropic multivariate Gaussian distributions: labels Y were sampled from $Y \sim N(0, I_{10})$, and the examples for each label sampled from $X|Y \sim N(Y, \sigma^2 I_{10})$. The noise-level parameter σ determines the difficulty of classification. Similarly to the real-data example, we consider a 1-nearest neighbor classifier, which is given a single training instance per class.

For the estimation, we use the cross-validation procedure described in section 3.4 to select the parameter h of the "radial basis"

$$h_\ell(u) = \Phi\left(\frac{\Phi^{-1}(u) - t_\ell}{h}\right).$$

where t_ℓ are a set of regularly spaced knots which are determined by h and the problem parameters. Additionally, we add a constant element to the basis, equivalent to adding an intercept to the linear model (12).

The rationale behind the radial basis is to model the density of $\Phi^{-1}(U^*)$ as a mixture of gaussian kernels with variance h^2. To control overfitting, the knots are separated by at least a distance of $h/2$, and the largest knots have absolute value $\Phi^{-1}(1 - \frac{1}{rk_1^2})$. The size of the maximum knot is set this way since rk_1^2 is the number of ranks that are calculated and used by our method. Therefore, we do not expect the training data to contain enough information to allow our method to distinguish between more than rk_1^2 possible accuracies, and hence we set the maximum knot to prevent the inclusion of a basis element that has on average a higher mean value than $u = 1 - \frac{1}{rk_1^2}$. However, in simulations we find that the performance of the basis depends only weakly on the exact positioning and maximum size of the knots, as long as sufficiently large knots are included; the bandwidth h is the most crucial parameter. In the simulation, we use a grid $h = \{0.1, 0.2, \ldots, 1\}$ for the cross-validated selection of the bandwidth.

Comparison to Kay

In their paper[3], Kay et al. (2008) proposed a method for extrapolating classification accuracy to a larger number of classes. The method depends on repeated kernel-density estimation (KDE) steps. Because the method is only briefly motivated in the original text,

2. Alternatively, one could also evaluate predictions for all points in the held-out data, but due to correlation, this makes only a minor difference to the result.
3. page 29 of supplement to Kay et al. (2008)

k_1	k_2	CV-reg	KDE-BCV	KDE-UCV
500	1000	**0.032** (0.001)	0.090 (0.001)	0.067 (0.001)
500	2000	**0.044** (0.002)	0.088 (0.001)	0.059 (0.001)
500	5000	0.073 (0.004)	0.079 (0.001)	**0.051** (0.001)
500	10000	0.098 (0.004)	0.076 (0.001)	**0.045** (0.001)
5000	10000	**0.009** (0.000)	0.038 (0.000)	0.028 (0.000)
5000	20000	**0.015** (0.001)	0.028 (0.000)	0.019 (0.000)
5000	50000	**0.032** (0.002)	0.035 (0.000)	0.053 (0.000)
5000	100000	**0.054** (0.003)	0.065 (0.000)	0.086 (0.000)

Table 1: Maximum RMSE (se) across all signal-to-noise-levels in predicting TA_{k_2} from k_1 classes in multivariate gaussian simulation. Standard errors were computed by nesting the maximum operation within the bootstrap, to account for added variance from selection.

we present it in our notation. It is perhaps worthwhile to compare this to their original presentation.

For k_1 observed classes, let $m_{y_j}(x_i)\, 1 \leq i, j \leq k_1$ be the observed score comparing feature vector of the i'th class x_i to the label of the j'th class y_j. The KDE method proposes to estimate the density of scores for each distractor class using a Gaussian kernel function K $\hat{f}_i(m) = \frac{1}{k_1 - 1} \sum_{j \neq i} K(m_{y_i}(x_j), m)$. Probability of error against a single competitor is then computed for each class separately by integrating the density above the observed true score $m_{y_i}(x_i)$, in $h_2(i) = \int_{m_{y_i}(x_i)}^{\infty} \hat{f}(m) dm$. The probability of accurate classification of the i'th class against $k_2 - 1$ competitors is $h_{k_2}(i) = (1 - h(i))^{k_2 - 1}$. The average over the k_1 classes is the estimated generalization accuracy $\hat{AGA}_{KDE} = \frac{1}{k_1} \sum_i^{k_1} h_{k_2}(i)$.

Note that the method depends heavily on the density estimation step. If the kernel bandwidth is too small compared to the number of classes, the extrapolated accuracy will be upwardly biased. To see this, consider a class i that is correctly classified in the original class set. That is, $m_{y_i}(x_i) > m_{y_j}(x_i)$ for every $j \neq i$. If we use for $\hat{f}_i$ the unsmoothed empirical density, $h_2(i)$ will be 1 and therefore $h_{k_2}(i)$ will be 1 as well. In other words, the method relies on smoothing of each class to generate a the tail density that exceeds $m_{y_i}(x_i)$, and therefore it is highly dependent on the choice of kernel bandwidth.

In our simulation, we tested our own implementation of the KDE method, using the two methods for cross-validated KDE estimation provided in the `stats` package in the `R` statistical computing environment: biased cross-validation and unbiased cross-validation (Scott, 1992).

Simulation Results

We see in 7 that the cross-validated regression method (CV-reg) and the KDE methods with unbiased and biased cross-validation (KDE-UCV, KDE-BCV) perform comparably in the gaussian simulations. Within each problem setting defined by the number of source and target classes (k_1, k_2), we use the maximum RMSE across all signal-to-noise settings to quantify the overall performance of the method, as displayed in Table 1.

We studied how the difficulty of extrapolation relates to both the absolute size of the number of classes and the factor of increase from the source number of classes k_1 to the target number of classes k_2. Our simulation has two settings for $k_1 = \{500, 5000\}$, and within each setting we have extrapolations to 2 times, 4 times, 10 times, and 20 times the number of classes. The results indicate that the difficulty mainly depends on the extrapolation factor $\frac{k_2}{k_1}$, although different methods show different sensitivities to the absolute number of classes. The cross-validated regression method improves in worst-case RMSE when moving from $k_1 = 500$ to $k_1 = 5000$ while keeping the factor of increase fixed, most dramatically in the case $\frac{k_2}{k_1} = 2$ when it improves from a maximum RMSE of 0.032 ± 0.001 to 0.009 when going from $k_1 = 500$ to $k_1 = 5000$, which is 3.5-factor reduction in worst-case RMSE, but also gaining at least a 1.8-factor reduction in RMSE when going from the smaller problem to the larger problem in the other three cases. KDE-BCV also improves in worst-case RMSE when going from 500 to 5000 training classes while keeping the extrapolation factor fixed, but KDE-UCV breaks the pattern, slightly increasing in worst-case RMSE for extrapolation factor $\frac{k_2}{k_1} = 10$, from 0.051 ± 0.001 to 0.053, and greatly increasing for $\frac{k_2}{k_1} = 20$, from 0.045 ± 0.001 to 0.086. While collecting more simulation data points would be helpful in confirming these trends, the results suggest that both CV-reg and KDE-BCV benefit from having more data to tune its bandwidth parameter. In theory, KDE-UCV should also enjoy the same benefit of having more data to tune the kernel bandwidth, but other effects may lead to its loss of calibration in larger extrapolation problems, as we shall discuss.

Inspecting the curves in Figure 7, we see that the RMSE curves of KDE-BCV and KDE-UCV vary more smoothly with respect to the signal-to-noise ratio (and hence true target accuracy) than CV-reg, which looks quite jagged. From simulation studies where we fixed the bandwidth of the regression method, we see that the roughness is an intrinsic property of the regression method with a finite basis set rather than a consequence of the discontinuity of bandwidth selection. This can be explained by the fact that the set of possible fits of the regression model to the training data are constrained to a polyhedral cone, as we will elaborate in the discussion.

If we look at the mean predicted accuracy versus the true accuracy for the simulations, displayed in Figure 8, we see that the CV regression method has less overall bias than the KDE methods for both the small and large extrapolation problems. This can be explained as a consequence of the intrinsic bias in the KDE extrapolation method, which we also elaborate upon in the discussion.

5. Experimental Evaluation

We demonstrate the extrapolation of average accuracy in two data examples: (i) predicting the accuracy of a face recognition on a large set of labels from the system's accuracy on a smaller subset, and (ii) extrapolating the performance of various classifiers on an optical character recognition (OCR) problem in the Telugu script, which has over 400 glyphs.

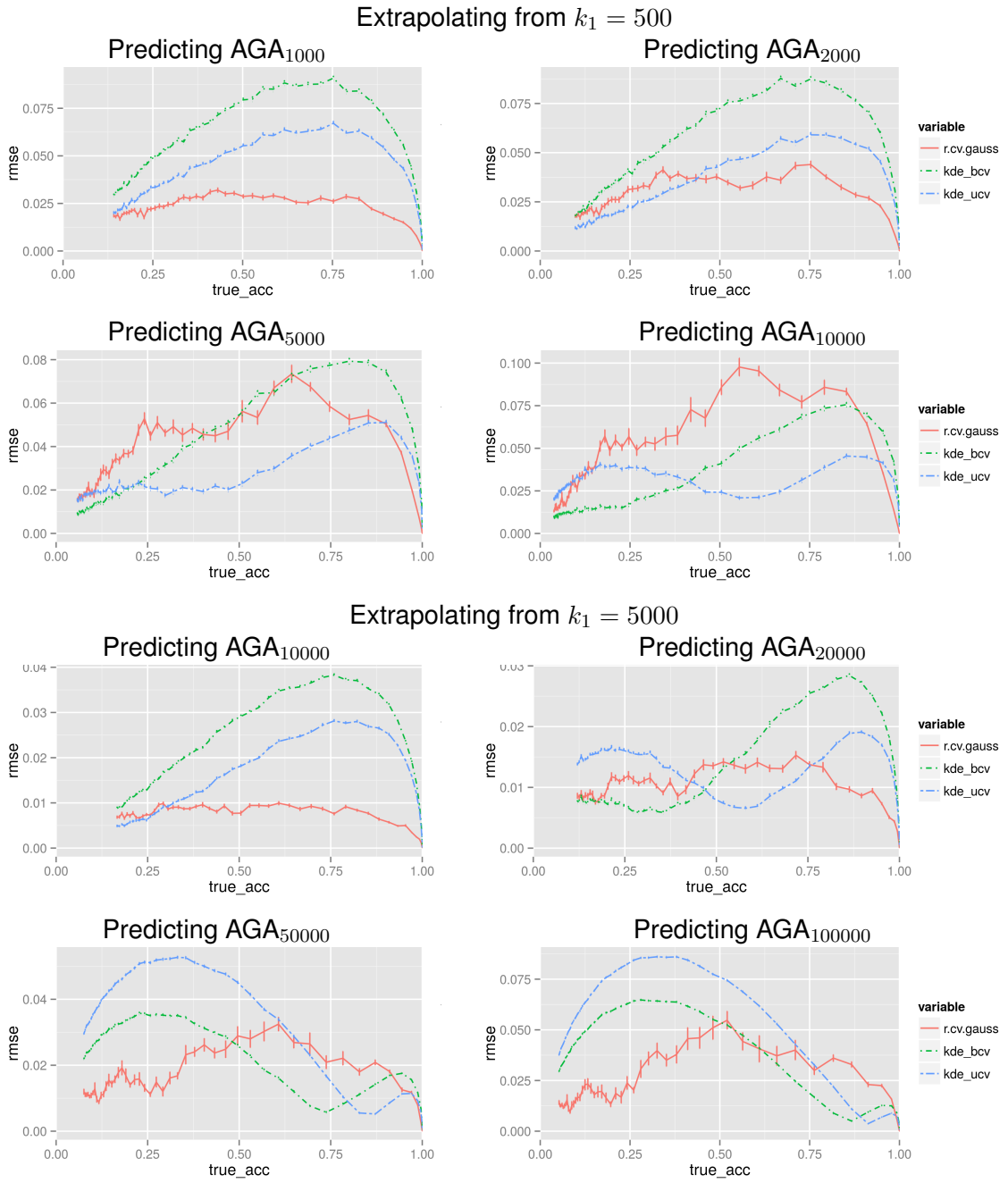

Figure 7: **Simulation results (RMSE):** Simulation study consisting of multivariate Gaussian Y with nearest neighbor classifier. Prediction RMSE vs true k_2-class accuracy for cross-validated regression method with radial basis (`r.cv.gauss`), KDE-based methods with biased cross-validation (`kde_bcv`) and unbiased cross-validation (`kde_ucv`).

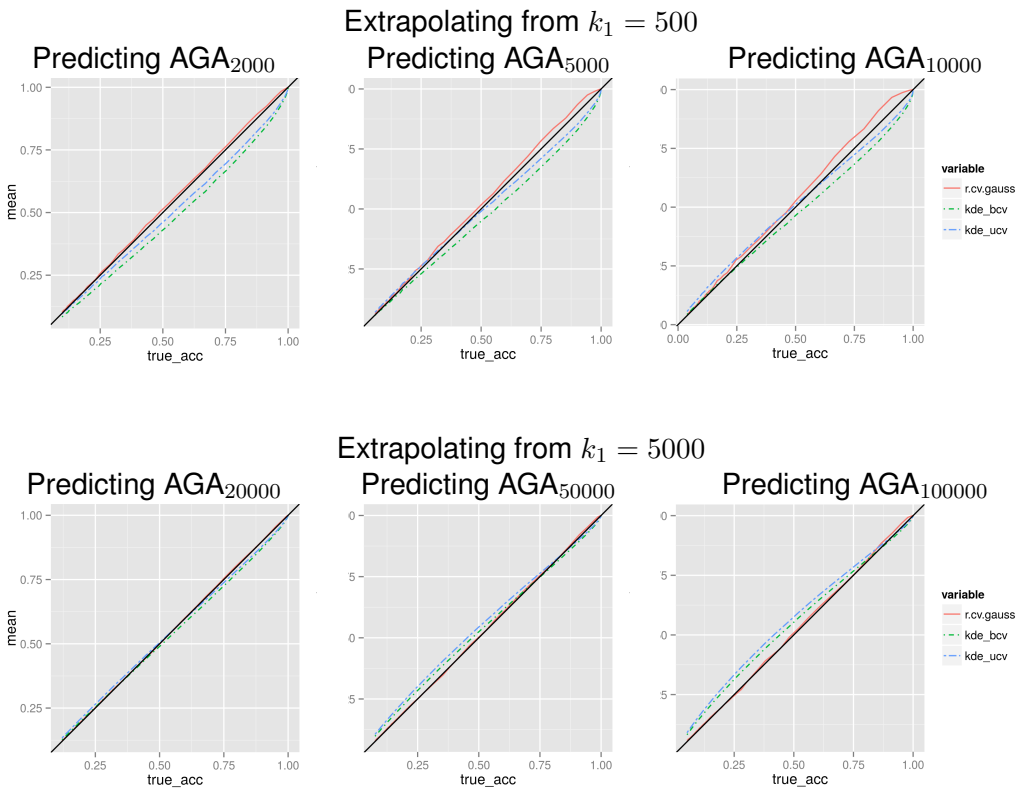

Figure 8: **Simulation results (biases):** Simulation study consisting of multivariate Gaussian Y with nearest neighbor classifier. Mean predicted accuracy vs true k_2-class accuracy for cross-validated regression method with radial basis (`r.cv.gauss`), KDE-based methods with biased cross-validation (`kde_bcv`) and unbiased cross-validation (`kde_ucv`).

Label	Training			Test
$y^{(1)}$=Amelia	$x_1^{(1)}$ = 	$x_2^{(1)}$ = 	$x_3^{(1)}$ = 	$x_*^{(1)}$ = 
$y^{(2)}$=Jean-Pierre	$x_1^{(2)}$ = 	$x_2^{(2)}$ = 	$x_3^{(2)}$ = 	$x_*^{(2)}$ = 
$y^{(3)}$=Liza	$x_1^{(3)}$ = 	$x_2^{(3)}$ = 	$x_3^{(3)}$ = 	$x_4^{(3)}$ = 
$y^{(4)}$=Patricia	$x_1^{(4)}$ = 	$x_2^{(4)}$ = 	$x_3^{(4)}$ = 	$x_4^{(4)}$ = 

Figure 9: **Face recognition setup:** Examples of labels and features from the *Labeled Faces in the Wild* dataset.

5.1 Face recognition

Data

From the "Labeled Faces in the Wild" dataset (Huang et al. (2007)), we selected the 1672 individuals with at least 2 face photos. We form a dataset consisting of photo-label pairs $(x_j^{(i)}, y^{(i)})$ for $i = 1, \ldots, 1672$ and $j = 1, 2$ by randomly selecting 2 face photos for each individual.

Classifier

We implement a two-step face recognition system based on a precomputed neural-network based embedding followed by a one nearest neighbor classifier.

We used the OpenFace (Amos et al. (2016)) embedding for feature extraction. For each photo x, a 128-dimensional feature vector $g(x)$ is obtained as follows. The computer vision library DLLib is used to detect landmarks in x, and to apply a nonlinear transformation to align x to a template. The aligned photograph is then downsampled to a 96×96 image. The downsampled image is fed into a pre-trained deep convolutional neural network to obtain the 128-dimensional feature vector $g(x)$. More details are found in (Amos et al. (2016)).

The recognition system then works as follows. Suppose we want to perform facial recognition on a subset of the individuals, $I \subset \{1, \ldots, 1672\}$. Then, for all $i \in I$, we load one example-label pair, into the system, $(x_1^{(i)}, y^{(i)})$. In order to identify a new photo $\tilde{z}^*$, we obtain the feature vector $g(x^*)$, and guess the label $\hat{y}$ with the minimal Euclidean distance between $g(y^{(i)})$ and $g(x^*)$, which implies a score function

$$M_{y^{(i)}}(x^*) = -||g(x_1^{(i)}) - g(x^*)||^2.$$

The test accuracy is assessed on the unused repeat for all individuals in I. Note that the assumptions of our estimation method are met in this example because one-nearest neighbor is a marginal classifier. We note that m-nearest neighbor for $m > 1$ is not marginal.

Experimental Details

We treat the full data-set of 1672 as our population of labels. In each experiment, we choose a random subset of size $k_1 < 1672$, for which we observe both training and test

data. From this data, we will estimate AGA_{k_2} for k_2 between $k_2 = k_1 + 1, ..., 1672$. We use $k_1 = 100, 200, 400, 800$, with $B = 300$ repeats for each subset size.

For the selected subset of size k_1, we can estimate the test accuracy at every $k \leq k_1$, getting the vector $(\text{ATA}_2, ..., \text{ATA}_{k_1})$. Specifically, we use a linear spline basis,

$$h_\ell(u) = \left[u - \frac{\ell}{m+1}\right]_+$$

for $\ell = 1, \ldots, m$. Here we take $m = 10000$. We fit the β coefficient vector using non-negative least squares:

$$\hat{\beta} = \text{argmin}_{\beta:\beta_\ell \geq 0} \sum_{k=2}^{k_1} \left((1 - \text{ATA}_k) - \sum_{\ell=1}^{m} \beta_\ell H_{\ell,k} \right)^2$$

The non-negativity constraint on the coefficients β, combined with the linear spline basis, ensures that $D(u)$ is a monotonic and convex function on $[0, 1]$.

Based on the β coefficients, we can compute the prediction for the full dataset $\hat{AGA}_{1672}$. We compare the prediction to the observed accuracy on full dataset TA_{1672}, which approximates the ground truth.

Results

The extrapolation results can be seen in Figure 10, which plots the extrapolated accuracy curves for each method for 100 different subsamples of size k_1. As can be seen, for all three methods, the variances decrease rapidly as k_1 increases. In general, for $k_1 > 400$ the paths of the different extrapolation curves are not very different.

The root-mean-square errors between at $k_2 = 1672$ can be seen in Table 2. KDE-BCV achieves the best extrapolation for all three cases $k_1 = \{100, 200, 400\}$ with KDE-UCV consistently achieving second place. These results differ from the ranking of the RMSEs for the analagous simulation when predicting $k_2 = 2000$ from $k_1 = 500$ for accuracies around 0.45: in the first row and second column of Figure 7, where the true accuracy is 0.43 (from setting $\sigma^2 = 0.2$), the lowest RMSE belongs to KDE-UCV (RMSE=0.0361 ± 0.001), followed closely by CV-reg (RMSE=0.0372 ± 0.002), and KDE-BCV (RMSE=0.0635 ± 0.001) having the highest RMSE. These discrepancies could be explained by differences between the data distributions between the simulation and the face recognition example, and also by the fact that we only have access to the $k_2 = 1672$-class ground truth for the real data example. In simulations, we see that the empirical test accuracy for $k_2 = 1600$ classes and $r = 1$ repeats varies by a standard deviation of 0.01 in signal-to-noise settings with true accuracies around 0.4. Since the RMSEs of the simulation and the real-data example differ by a little more than 2 standard deviations, it is plausible that evaluating the methods with respect to the true population accuracy AGA_{1672} would yield a ranking that was consistent with the simulation.

5.2 Telugu OCR

We apply performance extrapolation in an optical character recognition example (Achanta and Hastie (2015)). We consider the use of three different classifiers: logistic regression,

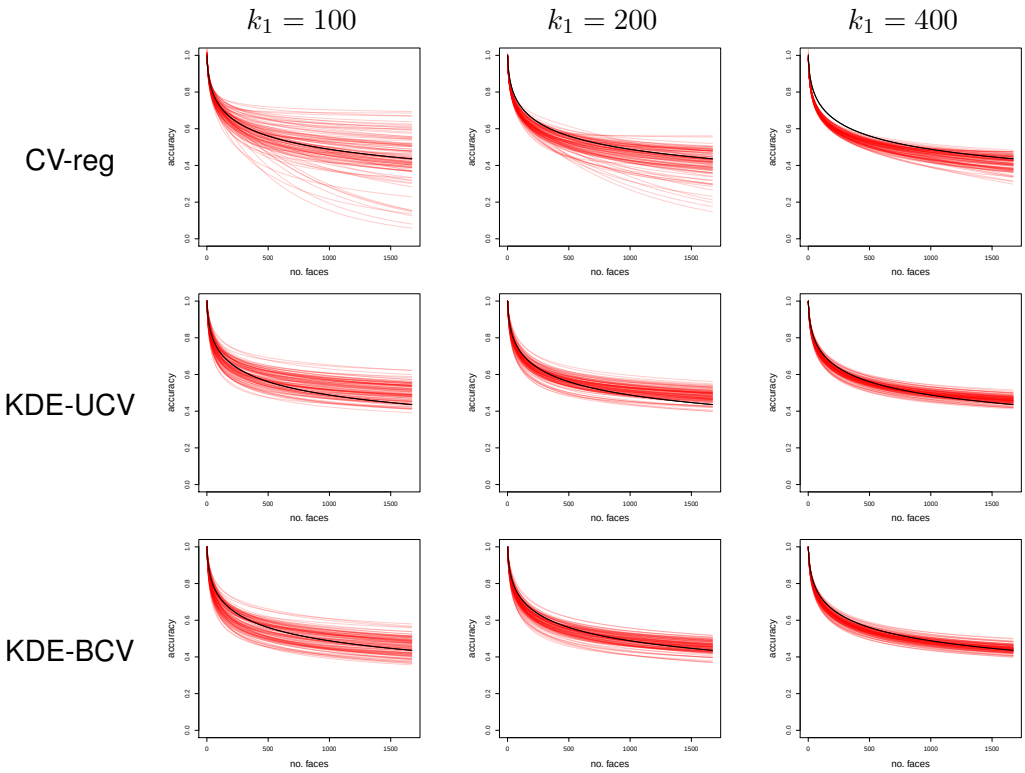

Figure 10: **Comparison of KDE and CV regression methods**: The plots show predicted accuracies using a different source dataset size k_1. Each red curve represents the estimated accuracies using a single subsample. The black curve shows the true average accuracy.

k_1	100	200	400
CV-reg	0.113 (0.002)	0.058 (0.002)	0.050 (0.001)
KDE-UCV	0.082 (0.001)	0.057 (0.001)	0.035 (0.001)
KDE-BCV	**0.053** (0.001)	**0.037** (0.001)	**0.024** (0.001)

Table 2: RMSE (se) on predicting TA_{1672} from k_1 classes

k_1	k_2	Classifier	True	KDE-BCV	KDE-UCV	CV-reg
20	100	Deep CNN	0.9908	0.7138	0.6507	**0.9905**
		Logistic	0.8490	**0.8414**	0.8161	0.8980
		SVM	0.7582	0.6544	0.5771	**0.8192**
20	400	Deep CNN	0.9860	0.4903	0.3863	**0.9614**
		Logistic	0.7107	0.7467	**0.7015**	0.8824
		SVM	0.5452	**0.5163**	0.4070	0.6725
100	400	Deep CNN	0.9860	0.8910	0.8625	**0.9837**
		Logistic	0.7107	**0.7089**	0.6776	0.7214
		SVM	0.5452	0.4369	0.3528	**0.5969**

Table 3: Extrapolating from k_1 to k_2 classes in Telugu OCR for three different classifiers: logistic regression, support vector machine, and deep convolutional network

linear support-vector machine (SVM), and a deep convolutional neural network[4]. The full data consists of 400 classes with 50 training and 50 test observations for each class. We also create a nested hierarchy of subsampled data consisting of (i) a subset of size 100 randomly sampled from the 400 classes, and (ii) yet another subsampled dataset consisting of 20 classes random subsampled from the size-100 subsample. We therefore study three different prediction extrapolation problems:

1. Predicting the accuracy on $k_2 = 100$ classes from $k_1 = 20$ classes, comparing the predicted accuracy to the test accuracy of the classifier on the 100-class subsample as ground truth.

2. Same as (1), but setting $k_2 = 400$ and $k_1 = 20$, and using the full dataset for the ground truth.

3. Same as (2), but setting $k_2 = 400$ and $k_1 = 100$.

Note that unlike in the case of the face recognition example, here the assumption of marginal classification is satisfied for none of the classifiers. We compare the result of our model to the ground truth obtained by using the full dataset.

The results are displayed in table 3. If we rank the three extrapolation methods in terms of distance to the ground truth accuracy, we see a consistent pattern of rankings between the 20-to-100 extrapolation and the 100-to-400 extrapolation. As we remarked in the simulation, the difficulty of extrapolation appears to be primarily sensitive to the extrapolation ratio $\frac{k_2}{k_1}$, which are similar (5 versus 4) in the 20-to-100 and 100-to-400 problems. In both settings, CV regression comes closest to the ground truth for the Deep CNN and the SVM, but KDE-BCV comes closest to ground truth for the Logistic regression. However, even for logistic regression, CV regression does better or comparably to KDE-UCV.

In the 20-to-400 extrapolation, which has the highest extrapolation ratio ($\frac{k_2}{k_1} = 20$), none of the three extrapolation methods performs consistently well for all three classifiers. It could be the case that the variability is a dominating effect given the small training

4. The network architecture is as follows: `48x48-4C3-MP2-6C3-8C3-MP2-32C3-50C3-MP2-200C3-SM`.

set, making it difficult to compare extrapolation methods using the 20-to-400 extrapolation task.

Unlike in the face recognition example, we did not resample training classes here, because that would require retraining all of the classifiers–which would be prohibitively time-consuming for the Deep CNN. Thus, we cannot comment on the robustness of the comparisons from this example, though it is likely that we would obtain different rankings under a new resampling of the training classes.

6. Discussion

In this work, we suggest treating the class set in a classification task as random, in order to extrapolate classification performance on a small task to the expected performance on a larger unobserved task. We show that average generalized accuracy decreases with increased class-set size like the $(k-1)$th moment of a distribution function. Furthermore, we introduce an algorithm for estimating this underlying distribution, that allows efficient computation of higher order moments. There are many choices and simplifying assumptions used in the description of the method. In this discussion, we discuss these decisions and map some alternative models or strategies for future work.

Comparison to Kay et al.

The extrapolation method of Kay et al. (2008) can be described in our framework as follows. Let F_x be the cumulative distribution function of $M_{Y'}(x)$ for a random label $Y' \sim \pi$. For each test instance $x_j^{(i)}$, let $\hat{F}_{x_j^{(i)}}(m_{y^{(i)}}(x_j^{(i)}))$ be an estimate of $F_{x_j^{(i)}}(m_{y^{(i)}}(x_j^{(i)}))$. The particular estimation method recommended by Kay et al. (2008) is to estimate the density $f_{x_j^{(i)}}$ by using kernel-density estimation with a Gaussian kernel and a bandwidth chosen via pseudolikelihood cross-validation (Cao et al., 1994); however, our criticism is not specific to the use of a particular estimator for $\hat{F}_x$. Extrapolate using the formula

$$\widehat{\mathrm{AGA}_k} = \frac{1}{k_1 r} \sum_{i=1}^{k} \sum_{j=1}^{r} \hat{F}_{x_j^{(i)}}(m_{y^{(i)}}(x_j^{(i)}))^{k-1}$$

While no justification is given for the method in Kay et al. (2008), one possible justification is the fact that

$$\mathrm{AGA}_k = \mathbf{E}[F_X(M_Y(X))^{k-1}].$$

Therefore, the method can give good extrapolations when the estimated probabilities $\hat{F}_{x_j^{(i)}}(m_{y^{(i)}}(x_j^{(i)}))$ are close to the true probabilities $F_{x_j^{(i)}}(m_{y^{(i)}}(x_j^{(i)}))$. However, the method ignores the bias introduced by exponentiation. That is, even if $\hat{p}$ is an unbiased estimator of p, $\hat{p}^k$ may *not* be a very good estimate of p^k, since

$$p^k = \mathbf{E}[\hat{p}]^k \neq \mathbf{E}[\hat{p}^k].$$

unless $\hat{p}$ is a degenerate random variable (constant). Otherwise, for large k, $\hat{p}^k$ may be an extremely biased estimate of p. Our proposed method avoids this source of bias by

estimating the $(k-1)$st moment of $D(u)$ directly. As we see in Figure 8, correcting for the bias of exponentiation helps greatly to reduce the overall bias, although some residual bias for the regression method still remains due to the nonnegativity constraint on the coefficients and model mispecification.

Behavior of RMSE curves

As we saw in 7, the error curves of the KDE method vary much more smoothly than the regression method with respect to changes in the parameters of the data distribution. In the multivariate gaussian simulation, as the distribution of the training data moves within (k_1-1)-dimensional space, the projection of the mean of the data distribution onto the cone traces out a piecewise smooth curve as the signal-to-noise parameter σ for generating the data is varied. This observation suggests that carefully adjusting the placement of the basis knots could improve the worst-case goodness-of-fit to the multivariate gaussian model (or any parametric data model) by flattening out the "peaks" seen in Figure 7, but we leave this idea to future work.

Marginal classifiers

One limitation of our analysis of average accuracy is that it applies only to marginal classifiers. Theoretically, it may be possible to extend the analysis to certain non-marginal classifiers, for instance, by showing that in the large-k limit such classifiers become "asymptotically" marginal, in some sense. Furthermore, there is no obstacle in testing the extrapolation method to see how well it would recover accuracy curves for non-marginal classifiers.

Sampling

Our analysis is currently restricted to randomized classification problems with i.i.d. sampling of classes. Extension to other sampling mechanisms, such as cluster sampling, may be possible if one can work out how the dependence between classes translates into dependence between the favorabilities $U_{X^*}(m_{Y^{(k)}})$.

More broadly, the assumption that the labels in $\mathcal{S}_k$ are a random sample from a distribution π may be inappropriate. Many natural classification problems arise from hierarchically partitioning a space of instances into a set of labels. Therefore, rather than modeling $\mathcal{S}_k$ as a random sample, it may be more suitable to model it as a random hierarchical partition of $\mathcal{Y}$ (for instance, arising from an optional Pólya tree process, Wong et al. (2010)). Finally, note that we assume no knowledge about the new class-set except for its size. Better accuracy might be achieved if some partial information is known.

Arbitrary cost functions

In the current paper, we only discussed extrapolating the classification accuracy–or equivalently, the risk for the zero-one cost function. However, it is possible to extend our analysis to risk functions with arbitrary cost functions, which is the subject of forthcoming work.

Predicting the generalization accuracy

In this work, our focus was on estimating the average generalization accuracy. However, rather being interested in the average accuracy for a new label set, one might be interested in predicting the generalization accuracy on a particular problem. When the source task and target tasks are independent, then the average generalization accuracy is also Bayes estimate which minimizes mean-squared prediction error. However, it may be known that there is overlap between the labels or data used in the source task or target task. Conditioning on this information may yield a more accurate prediction. However, we leave this problem to future work.

Confidence and prediction intervals

In many of the applications discussed in the introduction, it would be useful to construct either confidence intervals for the average generalization accuracy AGA_k, or prediction intervals for the generalization accuracy, GA_k. The key to constructing such intervals is to understand the variability properties of the inputs to our estimation procedure, the average test accuracies ATA_k. We discuss the issue of constructing confidence and prediction intervals in forthcoming work.

Other transfer learning setups

In our analysis, we also limited the training set sizes to be the same in both the source and target tasks. It would be very nice to be able to relax this assumption, since in most practical applications, the training set sizes are varied within label sets as well as between tasks. The idea of extrapolating from learning curves (Cortes et al., 1994) may be one way to adjust for varying training set sizes.

Many other aspects of transfer learning could also be considered in conjunction with the issue of transferring from one label set to another, such as transfer to a different domain, or transfer to a target task without training data (Pan and Yang, 2010).

Acknowledgments

We thank Jonathan Taylor, Trevor Hastie, John Duchi, Steve Mussmann, Qingyun Sun, and Robert Tibshirani for useful discussion. CZ is supported by an NSF graduate research fellowship, and would also like to thank the European Research Council under the ERC grant agreement n°[PSARPS-294519] for travel support.

References

Felix Abramovich and Marianna Pensky. Feature selection and classification of high-dimensional normal vectors with possibly large number of classes. *arXiv preprint arXiv:1506.01567*, 2015.

Rakesh Achanta and Trevor Hastie. Telugu ocr framework using deep learning. *arXiv preprint arXiv:1509.05962*, 2015.

Brandon Amos, Bartosz Ludwiczuk, and Mahadev Satyanarayanan. Openface: A general-purpose face recognition library with mobile applications. Technical report, CMU-CS-16-118, CMU School of Computer Science, 2016.

Ricardo Cao, Antonio Cuevas, and Wensceslao González Manteiga. A comparative study of several smoothing methods in density estimation. *Computational Statistics & Data Analysis*, 17(2):153–176, 1994.

Corinna Cortes, Lawrence D Jackel, Sara A Solla, Vladimir Vapnik, and John S Denker. Learning curves: Asymptotic values and rate of convergence. In *Advances in Neural Information Processing Systems*, pages 327–334, 1994.

Koby Crammer and Yoram Singer. On the algorithmic implementation of multiclass kernel-based vector machines. *Journal of machine learning research*, 2(Dec):265–292, 2001.

Justin Davis, Marianna Pensky, and William Crampton. Bayesian feature selection for classification with possibly large number of classes. *Journal of Statistical Planning and Inference*, 141(9):3256–3266, 2011.

Jia Deng, Alexander C Berg, Kai Li, and Li Fei-Fei. What does classifying more than 10,000 image categories tell us? In *European conference on computer vision*, pages 71–84. Springer, 2010.

Jeff Donahue, Yangqing Jia, Oriol Vinyals, Judy Hoffman, Ning Zhang, Eric Tzeng, and Trevor Darrell. Decaf: A deep convolutional activation feature for generic visual recognition. In *International conference on machine learning*, pages 647–655, 2014.

Pinar Duygulu, Kobus Barnard, Joao FG de Freitas, and David A Forsyth. Object recognition as machine translation: Learning a lexicon for a fixed image vocabulary. In *European conference on computer vision*, pages 97–112. Springer, 2002.

Gregory Griffin, Alex Holub, and Pietro Perona. Caltech-256 object category dataset. 2007.

Maya R Gupta, Samy Bengio, and Jason Weston. Training highly multiclass classifiers. *Journal of Machine Learning Research*, 15(1):1461–1492, 2014.

Trevor Hastie, Robert Tibshirani, and Jerome Friedman. *The Elements of Statistical Learning*, volume 1. Springer, 2 edition, 2009. ISBN 9780387848570. doi: 10.1007/b94608. URL `http://www.springerlink.com/index/10.1007/b94608`.

Gary B. Huang, Manu Ramesh, Tamara Berg, and Erik Learned-Miller. Labeled faces in the wild: A database for studying face recognition in unconstrained environments. Technical Report 07-49, University of Massachusetts, Amherst, October 2007.

Kendrick N Kay, Thomas Naselaris, Ryan J Prenger, and Jack L Gallant. Identifying natural images from human brain activity. *Nature*, 452(March):352–355, 2008. ISSN 0028-0836. doi: 10.1038/nature06713.

Yoonkyung Lee, Yi Lin, and Grace Wahba. Multicategory support vector machines: Theory and application to the classification of microarray data and satellite radiance data. *Journal of the American Statistical Association*, 99(465):67–81, 2004.

Maxime Oquab, Leon Bottou, Ivan Laptev, and Josef Sivic. Learning and transferring mid-level image representations using convolutional neural networks. In *Proceedings of the IEEE conference on computer vision and pattern recognition*, pages 1717–1724, 2014.

Rui Pan, Hansheng Wang, and Runze Li. Ultrahigh-dimensional multiclass linear discriminant analysis by pairwise sure independence screening. *Journal of the American Statistical Association*, 111(513):169–179, 2016.

Sinno Jialin Pan and Qiang Yang. A survey on transfer learning. *IEEE Transactions on knowledge and data engineering*, 22(10):1345–1359, 2010.

D. W. Scott. *Multivariate Density Estimation: Theory, Practice, and Visualization*. Wiley, 1992.

C. E. Shannon. A Mathematical Theory of Communication. *Bell System Technical Journal*, 27(3):379–423, 1948. ISSN 00058580. doi: 10.1002/j.1538-7305.1948.tb01338.x. URL `http://ieeexplore.ieee.org/lpdocs/epic03/wrapper.htm?arnumber=6773024`.

Ali Sharif Razavian, Hossein Azizpour, Josephine Sullivan, and Stefan Carlsson. Cnn features off-the-shelf: an astounding baseline for recognition. In *Proceedings of the IEEE conference on computer vision and pattern recognition workshops*, pages 806–813, 2014.

Efstathios Stamatatos, Walter Daelemans, Ben Verhoeven, Patrick Juola, Aurelio López-López, Martin Potthast, and Benno Stein. Overview of the author identification task at pan 2014. In *CLEF (Working Notes)*, pages 877–897, 2014.

Roberto Togneri and Daniel Pullella. An overview of speaker identification: Accuracy and robustness issues. *IEEE Circuits and Systems Magazine*, 11(2):23–61, 2011.

Jason Weston, Chris Watkins, et al. Support vector machines for multi-class pattern recognition. In *ESANN*, volume 99, pages 219–224, 1999.

Wing H Wong, Li Ma, et al. Optional pólya tree and bayesian inference. *The Annals of Statistics*, 38(3):1433–1459, 2010.